



Design and fabrication of holographic optical elements for the generation of tilted and accelerating Airy beams

Raghu Dharmavarapu, A Vijayakumar and Shanti Bhattacharya
Center for NEMS and Nanophotonics, Department of Electrical Engineering,
Indian Institute of Technology Madras, Chennai Pin, , India

Dedicated to Padma Shree Prof R S Sirohi, FNAE

A modified perspective for the generation of tilted and accelerating Airy beams using computer generated holography is presented. The optical system simulated in computer for the generation of such beams consists of an axicon and a Beam Path Steering Element (BPSE). The axicon generates the zeroth order Bessel-like beam propagating along the optics axis while the BPSE converts the zeroth order Bessel-like beam into an accelerating beam. The beam path profile of the accelerating beam can be precisely engineered by accurate selection of the phase profile of the BPSE. The diffraction patterns of the element were simulated in the far field using Fraunhofer diffraction formula. The computer generated holographic optical elements were fabricated using electron beam direct writing. The evaluation results matched well with the simulation results. © Anita Publications. All rights reserved.

Keywords: Accelerating Airy beams, Bessel beam, Computer generated holography

1 Introduction

Beam shaping involves changing of the beam intensity and/or phase profile in order to create a light field that will be of more use in a particular application. Initial beam-shaping, as the name suggests redistributed the intensity uniformly into a different shape, e.g. the well-known flat-top beam [1, 2]. More sophisticated beam shaping includes the generation of optical beams like the Bessel and Laguerre-Gaussian, with special properties such as non-diffraction and angular momentum. Their use extended to the fields such as trapping and imaging [3,4], which in turn are used for measurement of various parameters.

Longitudinal beam shaping was used to shape the intensity of light along the propagation axis [5]. Snake like beams with tilt and slight acceleration were generated using Holographic Optical Elements (HOEs) [6]. In the recent past, the Airy beam has been added to the arsenal of beams with special properties. The observation of accelerating Airy beams was first reported in 2007 using cubic phase masks [7]. The most interesting property of an Airy beam is that their central lobe freely accelerates through space while maintaining the central spot size constant over reasonably long distances. They also exhibit self-healing, which means they can self-reconstruct even after being partially blocked by an obstacle. These properties of the Airy beams make them useful in applications such as optical particle trapping and guiding; and creating arbitrary curved plasma channels. The intensity profile of an Airy beam follows an Airy function, which is a solution of the paraxial equation given in Eq (1).

$$i \frac{\partial \phi}{\partial \xi} + \frac{1}{2} \frac{\partial^2 \phi}{\partial s^2} = 0,$$

ϕ represents the envelope of electric field. Equation (1) has an Airy non-dispersive solution [8], given in Eq (2).

$$\phi(\xi, s) = \text{Ai}(s - (\xi/2)^2) \exp(i(s\xi/2) - i(\xi^3/12)).$$

Here, $s = x/x_0$ represents a dimensionless transverse coordinate, x_0 is an arbitrary transverse scale, $\xi = z/kx_0^2$ is a normalized propagation distance, and $k = 2\pi n/\lambda_0$. When $\xi = 0$, Equation (2) becomes $\phi(0, s) = \text{Ai}(s)$. From Eq (2), we can see that the electric field envelope $\text{Ai}(s - (\xi/2)^2)$ shifts spatially as we move along the propagation (ξ) Type equation here.) direction. In this particular case, the beam follows a parabolic trajectory, as the spatial shift is a function of ξ^2

Corresponding author :

e-mail: physics.vijay@gmail.com (A Vijayakumar)

The mathematical formulation, design and generation of Airy beams have been discussed in various research papers [9-12]. In all the above, the design of the elements is cumbersome and the beams were generated using spatial light modulators. We believe that their potential in the field of metrology will be greatly enhanced if simpler techniques can be used to create the elements that will generate them. The elements can be fabricated using lithography, which will make them compact and easy to put into practical systems.

Therefore, in this paper, we propose a relatively simple procedure for design of holographic optical elements for the generation of Airy beams with any arbitrary beam path profile. The HOEs were fabricated using electron beam direct writing. The paper consists of four sections. In the first section, the design of the optical system and its analysis is presented. The design and simulation of HOEs and their respective diffraction patterns are discussed in the second section. The electron beam fabrication and optical testing are presented in the third and fourth sections, respectively.

2 Design of optical configuration

It is well known that when a parallel beam of light is incident on a refractive or a diffractive axicon, it generates a zeroth order Bessel-like beam within its focal depth and a ring pattern in its far field [12-14]. The optics configuration of the optical system containing an axicon and a Beam Path Steering Element (BPSE) is shown in Fig.1. Depending on whether a parallel glass plate (Fig 1), a thin prism (Fig 2) or a thin curved element (Fig. 3) were selected as the BPSE; either a zeroth order Bessel-like beam, a tilted Bessel-like beam or an Airy beam with a curved beam path profile will be generated, respectively.

Let α_1 be the base angle of the axicon and n_g be the refractive index of both the axicon and the BPSE. For case – 1 shown in Fig 1, the BPSE (a glass plate) introduces a constant phase to the wavefront and hence, the intensity profile and path are same as that of an independent axicon. In this case, the Bessel-like beam propagates in the same direction of z . The divergence angle β_1 is estimated using trigonometry as,

$$\beta_1 = \sin^{-1}(n_g \sin \alpha_1) - \alpha_1 \quad (3)$$

For smaller values of α_1 , the equation reduces to

$$\beta_1 = (n_g - 1) \alpha_1 \quad (4)$$

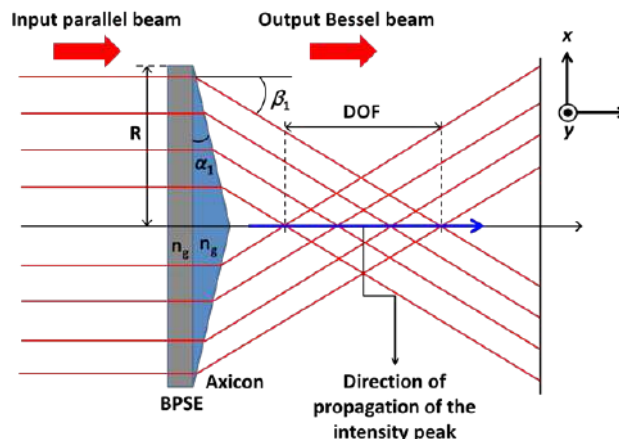


Fig 1. Optics configuration containing an axicon and a parallel glass plate as BPSE in tandem for the generation of Bessel-like beam

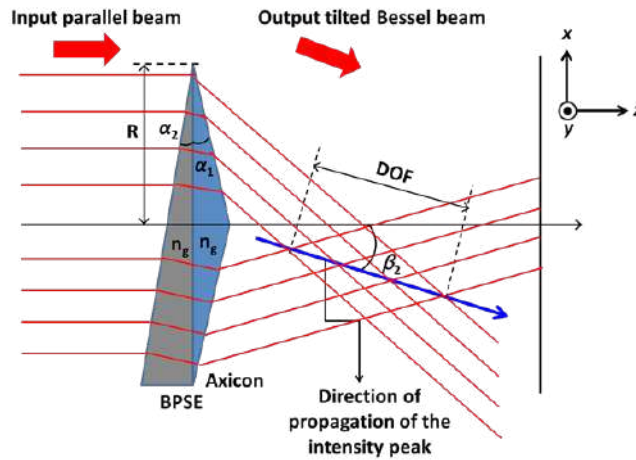


Fig 2 .Optics configuration containing an axicon and a thin prism as BPSE in tandem for the generation of tilted Bessel-like beam

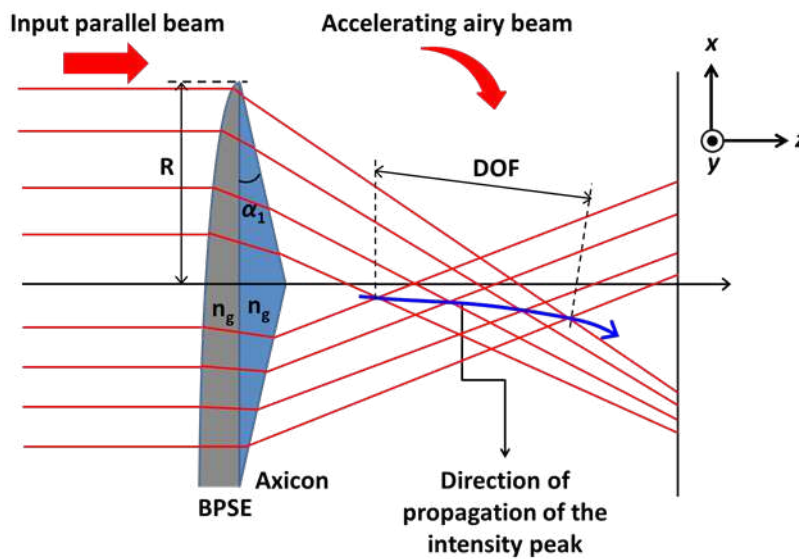


Fig 3. Optics configuration containing an axicon and a curved refractive element as BPSE in tandem for the generation of accelerating Airy beam

Considering a diffractive axicon, the diffraction angle β'_1 is given by [15,16]

$$\beta'_1 = \sin^{-1}((n_g - 1) \tan \alpha_1) \quad (5)$$

Equation (5) also reduces to Eq (4) for smaller values of α_1 . Hence, for both diffractive as well as refractive version of the axicon, for smaller angles of the axicon, the divergence angle remains same. The depth of focus (DOF) of the axicon is given by

$$DOF = R \tan \beta \quad (6)$$

For case – 2 shown in Fig 2, the BPSE (a thin prism) with an angle of α_2 and refractive index n_g is placed in tandem with the axicon. The axicon role in this configuration is to generate a zeroth order

Bessel-like beam while the thin prism is used to change the direction of the propagation of the zeroth order Bessel-like beam. The direction of propagation of the Bessel-like beam is given by

$$\beta_2 = \sin^{-1}(n_g \sin \alpha_2) - \alpha_2 \quad (7)$$

The thickness profile of the thin prism is of the form

$$t_1(x, y) = a_1 x + b_1 y, \quad (8)$$

where a_1 and b_1 are the coefficients of the thickness profile of the thin prism.

For case – 3, shown in Fig 3, the BPSE (a curved refractive element) is placed in tandem with the refractive axicon. In this case, the angles of the elements vary with (x, y) position. Hence, in this case, the angle α_2 is a function of position. This leads to a position dependent divergence angle $\beta_2(x, y)$ profile resulting in a curved path resembling the thickness profile of the BPSE. The thickness profile of the BPSE is given by

$$t_2(x, y) = f(x) + f(y) \quad (9)$$

The functions can be anything from polynomial to exponential functions. They can be selected based on the beam path requirement. From Figs 2 and 3, it can be seen that the thickness profile varying along the x -direction is transferred to the beam path profile along the z -direction. Hence, the thickness profile of the BPSE can be readily obtained from the required beam path profile of the Airy beam.

3 Design and simulation of holographic optical elements

Holographic optical elements are optical elements fabricated by interference between a plane wavefront and a wavefront with a special phase profile [17-19]. With the advent of computers, HOEs were easily created using software like Math CAD [20], MATLAB [21]. In this work, the HOEs were created using MATLAB by simulating the interference pattern between the conical wavefront generated by an axicon and the wavefront generated by the BPSE. The interference pattern was then binarized such that it could be fabricated using electron beam direct writing. The period of the axicon $\Lambda = 100 \mu\text{m}$. For case – 1, the constant phase profile of the BPSE is superposed with the phase profile of a conical beam. The phase profile of the resulting element before and after binarizing is shown in Fig 4(a) and Fig 4(b), respectively. The far field diffraction pattern of the binarized HOE is shown in Fig 4 (c). The binarization of the element leads to multiple diffraction orders [22] corresponding to its Fourier components.

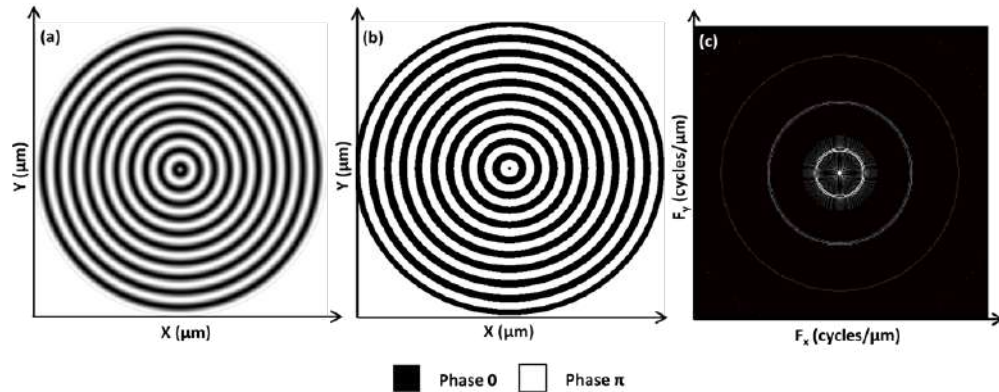


Fig 4. (a) Interference pattern obtained by superposition of a conical wavefront with a plane wavefront. (b) Binary holographic optical element used for the generation of Bessel-like beam when a plane wave is incident on it. (c) Far field diffraction pattern of the holographic optical element.

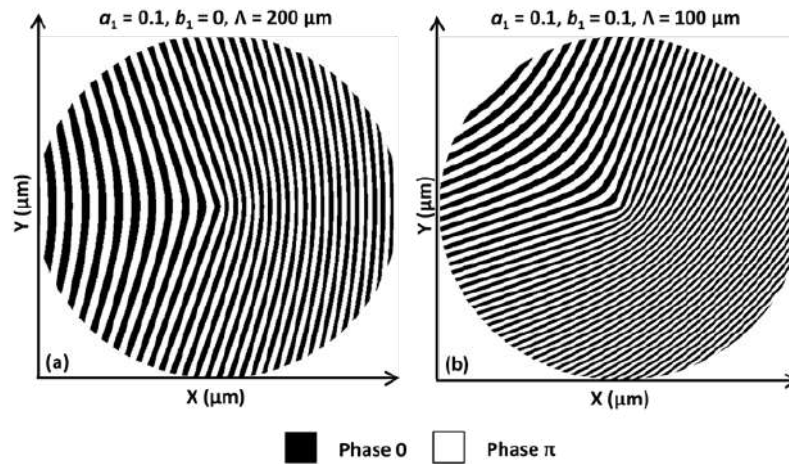


Fig 5. Binary holographic optical elements generated by the superposition of a tilted plane wavefront and a conical wavefront with (a) $a_1 = 0.1$, $b_1 = 0$, $\Lambda = 200 \mu\text{m}$, and (b) $a_1 = 0.1$, $b_1 = 0.1$, $\Lambda = 100 \mu\text{m}$, used for the generation of tilted Bessel-like beam when a plane wave is incident on it.

For case – 2, the linearly varying phase profile of the BPSE is superposed with the conical phase profile of the axicon. The coefficients were selected for two set of values of coefficients a_1 and b_1 . In the first case: $a_1 = 0.1$, $b_1 = 0$ and $\Lambda = 200 \mu\text{m}$ and in the second case: $a_1 = 0.1$, $b_1 = 0.1$ and $\Lambda = 100 \mu\text{m}$. The binarized versions of the interference patterns for these cases are shown in **Fig 5 (a)** and **(b)**, respectively. The element is generated by superposition of a tilted plane wavefront and a conical wavefront. When the element is illuminated using a plane wavefront, it generates a tilted Bessel-like beam [23]. However, due to binarization, two diffraction orders (± 1) will be generated with a maximum intensity of 40% each [22]. The far field diffraction patterns of **Fig 5 (a)** and **(b)** are shown in **Fig 6 (a)** and **(b)**, respectively.

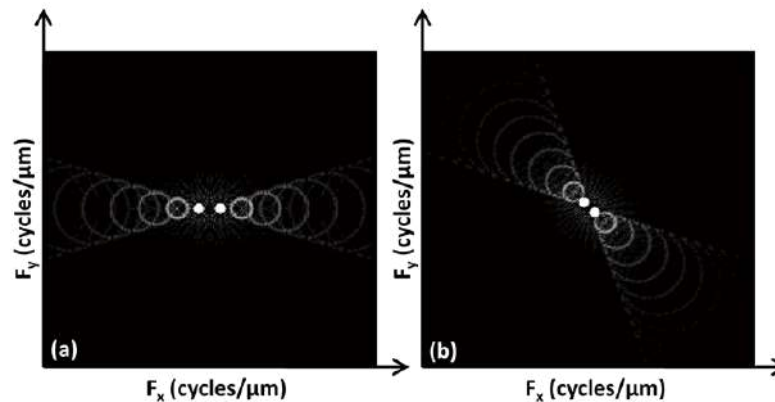


Fig 6. Far field diffraction pattern of the HOEs (a) $a_1 = 0.1$, $b_1 = 0$, $\Lambda = 200 \mu\text{m}$, and (b) $a_1 = 0.1$, $b_1 = 0.1$, $\Lambda = 100 \mu\text{m}$, used for the generation of tilted Bessel-like beam when a plane wave is incident on it.

A Bessel-like beam generated by a binary axicon transforms into a ring pattern in the far field [24]. Hence, the HOE generated by superposition of a tilted plane wavefront and a conical wavefront, generates a ring pattern off-axis. In this case, there are two dominant ring patterns (± 1) due to binarization. In the first case, the plane wavefront is tilted only along the x direction and hence the ring patterns occur along the F_x direction only. However, in the second case, the plane wavefront is tilted equally along both x as well as y directions resulting in the ring patterns occurring exactly at 45° with that of the $F_x - F_y$ plane.

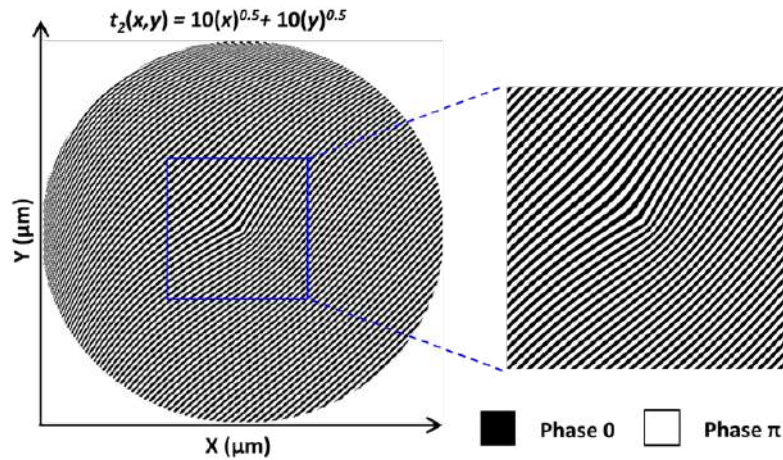


Fig 7. Binary HOE generated by the superposition of a curved plane wavefront and a conical wavefront with $t_2(x,y) = a_2(x)^{0.5} + b_2(y)^{0.5}$, used for the generation of accelerating Airy beam when a plane wave is incident on it.

For case – 3, a curved phase profile of the BPSE is superposed with the conical phase profile of the axicon. The functions along x and y axes were selected as $f(x) = a_2(x)^{0.5}$ and $f(y) = b_2(y)^{0.5}$, respectively, with thickness function $t_2(x,y) = a_2(x)^{0.5} + b_2(y)^{0.5}$. The coefficients a_2 and b_2 were selected to be 10 and the period of axicon $\Lambda = 100 \mu\text{m}$. The binarized version of the interference pattern for the case $a_2 = b_2 = 10$ is shown in Fig 7. The element is generated by superposition of a curved wavefront and a conical wavefront. Hence when the element is illuminated using a plane wavefront, it generates an accelerating Airy beam [25, 26]. However, due to binarization, two diffraction orders (± 1) will be generated with a maximum intensity of 40% each. The far field diffraction pattern of Fig 7 is shown in Fig 8.

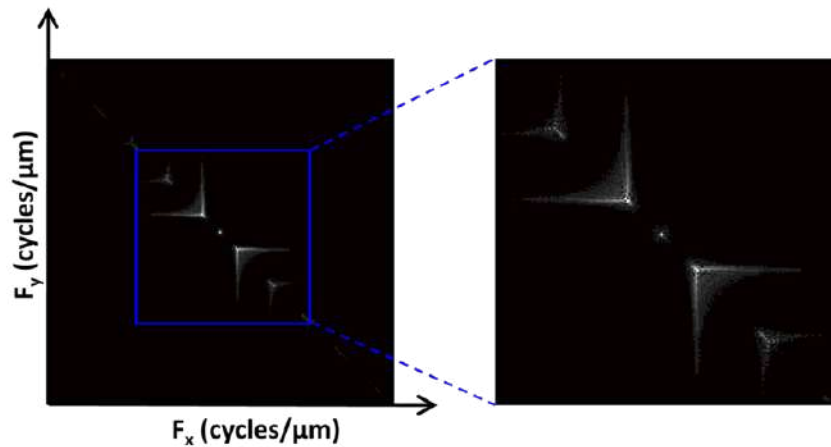


Fig 8. Far field diffraction pattern of the HOE generated by the superposition of a curved plane wavefront and a conical wavefront with $t_2(x,y) = a_2(x)^{0.5} + b_2(y)^{0.5}$.

4 Fabrication of HOEs

The HOEs designed were fabricated using a RAITH 150 TWO electron beam lithography system. Each HOE was designed with a diameter of 2 mm, for a wavelength of 633 nm and for the above design

values of HOEs. PMMA 950 K with 8% Anisole was used for fabrication. Borosilicate glass plates with ITO (Indium Tin Oxide) coating was used as substrate. The ITO layer prevents charging problem during electron beam writing. However, the presence of the ITO layer decreases the transmittivity to 85% for 633 nm. The refractive index of the resist is $n_r = 1.5$. The thickness of the resist required to obtain high efficiency of 40% in the $\pm 1^{\text{st}}$ diffraction order is given by $\lambda/2(n_r - 1) = 633 \text{ nm}$ for the above designed wavelength. The spin coating conditions and baking temperatures were optimized to obtain thickness of resist closer to the calculated value. A HMDS (Hexamethyldisilazane) is spin coated prior to the electron beam resist to improve adhesion between the resist and the substrate. MIBK (Methyl isobutyl ketone): IPA (Isopropyl alcohol) in the ratio of (1:3) was used for development (50 s) followed by cleaning with IPA (30 s) to remove the left over developer solution on the substrate.

The HOEs were fabricated with an electron beam dose of $70 \mu\text{C}/\text{cm}^2$, acceleration voltage of 10 kV and aperture of $30 \mu\text{m}$. The patterning time for each HOE was 1.5 hrs. The fabricated devices were imaged using a confocal microscope. The confocal microscope images of the fabricated devices for the generation of tilted Bessel-like beams for the cases ($a_1 = 0.1, b_1 = 0$) and ($a_1 = 0.1, b_1 = 0.1$) are shown in Fig 9 (a) and (b), respectively. The confocal microscope image of the central part of the HOE fabricated for the generation of accelerated Airy beam is shown in Fig 10.

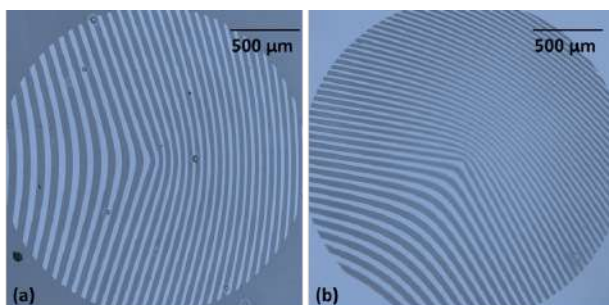


Fig 9. Confocal microscope images of the HOEs fabricated for the generation of tilted Bessel-like beams for the cases (a) ($a_1 = 0.1, b_1 = 0, \Lambda = 200 \mu\text{m}$) and (b) ($a_1 = 0.1, b_1 = 0.1, \Lambda = 100 \mu\text{m}$).

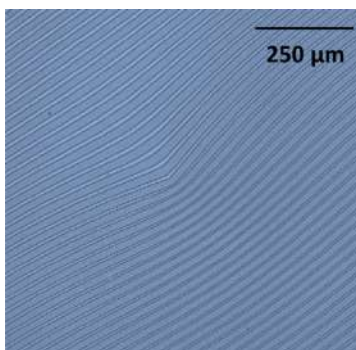


Fig 10. Confocal microscope image of the HOE with $t_2(x,y) = a_2(x)^{0.5} + b_2(y)^{0.5}$ fabricated for the generation of accelerating Airy beams.

5 Evaluation of HOEs

The fabricated elements were evaluated using He-Ne laser with a wavelength of 632.8 nm. The diffraction images were projected on to a screen and recorded using a camera. The far field diffraction

images of the HOEs used for the generation of tilted Bessel-like beams for the cases ($a_1 = 0.1, b_1 = 0$) and ($a_1 = 0.1, b_1 = 0.1$) are shown in Fig 11(a) and (b), respectively. The far field diffraction images of the HOE used for the generation of accelerating Airy beam with BPSE's thickness function $t_2(x,y) = a_2(x)^{0.5} + b_2(y)^{0.5}$ is shown in Fig 12.

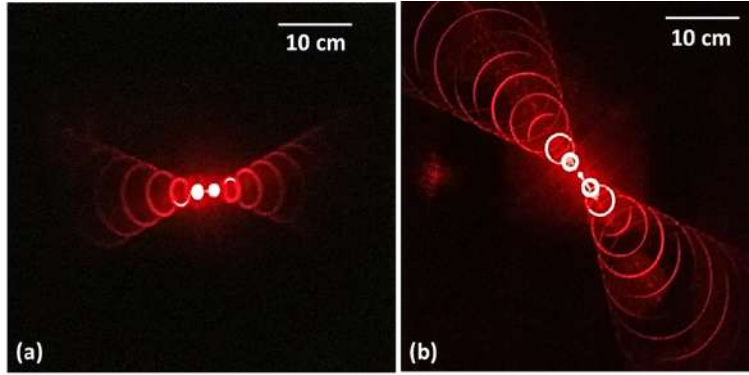


Fig. 11. Diffraction patterns of HOEs fabricated for the generation of tilted Bessel-like beams for the cases (a) ($a_1 = 0.1, b_1 = 0, \Lambda = 200 \mu\text{m}$) and (b) ($a_1 = 0.1, b_1 = 0.1, \Lambda = 100 \mu\text{m}$).

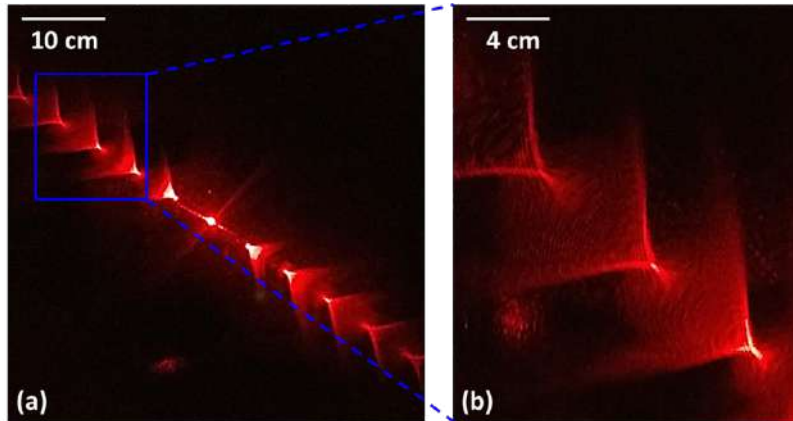


Fig 12. Diffraction patterns of HOE with $t_2(x,y) = a_2(x)^{0.5} + b_2(y)^{0.5}$ fabricated for the generation of accelerating Airy beams.

The experimental results seen in Figs 11 and 12 are in perfect agreement with the simulated results shown in Figs 6 and 8, respectively.

6 Conclusion

A modified approach for the design of HOEs for the generation of accelerating Airy beams is presented. An optical system consisting of two optical elements namely the axicon and the BPSE is used for the design of HOEs. BPSE can be precisely engineered to generate Airy beams with essential beam path. Two examples namely tilted Bessel-like beam and accelerated Airy beam with a specified beam path profile are discussed in this paper. All HOEs reported in this work, were fabricated as binary elements. Hence the incoming light is split into even and odd diffraction orders. The same procedure can be used to design and fabricate grey scale HOEs with only one diffraction order (+1 or -1) [14] with an efficiency > 90%.

This simple approach can be exploited for design of HOEs for the generation of Airy beams with any interesting beam path profile. The demonstrated technique is not just limited to Airy beams and can be easily extended to other types of beams like snake beams [6] by wise choice of the BPSE element. The above procedure can also be used for the design of micro refractive optical elements [26] namely axicon and BPSE which can be combined using epoxy and can be used for the generation of accelerating Airy beams.

Acknowledgements

The authors thank the Center for NEMS and Nanophotonics (CNNP) and associated faculty for the use of their equipment and fabrication facilities, as well as the Ministry of Communication and Information Technology (MCIT) for funding this project.

References

1. Tan X, Gu B-Y, Yang G-Z, Dong B-Z, *Appl Opt*, 34(1995)1314-1320.
2. Borek G T, Brown D R, *Proc SPIE*, 3633, Diffractive and Holographic Technologies, Systems, and Spatial Light Modulators VI, 51 (June 1, 1999).
3. Arlt J, Hitomi T, Dholakia K, *Appl Phys B*, 71(2000)549-554.
4. Zhang P, Goodwin P M, Werner J H, *Opt Express*, 22(2014)12398-12409.
5. Salik B, Rosen J, Yariv A, *J Opt Soc Am A*, 12(1995)1702-1706.
6. Rosen J, Yariv A, *Opt Lett*, 20(1995)2042-2044.
7. Siviloglou G A, Broky J, Dogariu A, Christodoulides D N, *Phys Rev Lett*, 99(2007)213901-213904.
8. Berry M V, Balazs N L, *Am J Phys*, 47(1979)264-267.
9. Zhao J, Zhang P, Deng D, Liu J, Gao Y, Chremmos I D, Efremidis N K, Christodoulides D N, Chen Z, *Opt Lett*, 4(2013)498-500.
10. Chremmos I D, Chen Z, Christodoulides D N, Efremidis N K, *Opt Lett*, 37(2012)5003-5005.
11. Hu Y, Siviloglou G A, Zhang P, Efremidis N K, Christodoulides D N, Chen Z, *Nonlinear Photonics and Novel Optical Phenomena, Springer Series in Optical Science*, 170(2012)1-46
12. Gao N, Li H, Zhu X, Hua Y, Xie C, *Opt Lett*, 38(2013)2829-2831.
13. McLeod J H, *J Opt Soc Am*, 44(1954)592-592.
14. Gervinskas G, Seniutinas G, Vijayakumar A, Bhattacharya S, Jelmakas E, Kadys A, Tomašiūnas R, Juodkasis S, in *Proc SPIE* 8923, Micro + Nano Materials, Devices, and Systems, 89234L (2013); doi: 10.1117/12.2033709.
15. Vijayakumar A, Bhattacharya S, *Opt Lett*, 37(2012)1980-1982.
16. Vijayakumar A, Bhattacharya S, *Opt Eng*, 54(2015)024104. doi:10.1117/1.OE.54.2.024104.
17. Vijayakumar A, Parthasarathi P, Iyengar S S, Selvan R, Ananthamurthy S, Bhattacharya S, *Proc SPIE*, 9654, (2015) 965426. doi:10.1117/12.2180850.
18. Chang B J, Leonard C D, *Appl Opt*, 18(1979)2407-2417.
19. Close D H, *Opt Eng*, 14(1975)145-402.
20. Sweatt W C, *J Opt Soc Am*, 67(1977)803-808.
21. Trester S, *Am J Phys*, 64(1996)472-478 .
22. Kim M K, *Opt Express*, 7(2000)305-310.
23. Kress B C, Meyrueis P, *Applied Digital Optics*, (John Wiley and Sons), 2009, p11.
24. Goodman J W, *Introduction to Fourier Optics*, (McGraw-Hill Series in Electrical and Computer Engineering), 1996, p 299.
25. Vijayakumar A, Bhattacharya S, *Appl Opt*, 53(2014)1979-1974.
26. Vo S, Fuerschbach K, Thompson K P, Alonso M A, Rolland J P, *J Opt Soc Am A*, 27(2010)2574-2582.

27. Yalizay B, Soyulu B, Akturk S, *J Opt Soc Am A*, 27(2010)2344-2346.

[Received: 8.7.2015; revised recd: 7.8.2015; accepted: 15.8.2015]

BIOGRAPHY OF AUTHORS

Raghu Dharmavarapu has obtained his Bachelor's degree in Electronics and Communications Engineering from Jawaharlal Nehru Technological University Hyderabad in 2012. He is currently pursuing his Master's degree under the guidance of Dr. Shanti Bhattacharya in the Photonics Group, Department of Electrical Engineering IIT Madras since 2014. He is currently working on fabrication of diffractive optical elements for beam shaping applications. Email: raghu1153@gmail.com



Dr. A Vijayakumar recently finished his Ph D titled, "Design, Fabrication and Evaluation of Diffractive Optical Elements for the generation of Focused Ring Patterns." This work was carried out at the Photonics Group, Department of Electrical Engineering, Indian Institute of Technology Madras. At present he continues to work there on the design and fabrication of composite diffractive optical elements. He will shortly be moving to Ben Gurion University, Israel, as a PBC outstanding post-doctoral fellow. Email: physics.vijay@gmail.com



Dr. Shanti Bhattacharya is part of the Photonics Group, Department of Electrical Engineering, IIT Madras, Department of Electrical Engineering, Indian Institute of Technology Madras. Her research interests include design, development and fabrication of novel diffractive optical elements, fiber based interferometry and optical MEMS. She is an editorial member of *Optik Journal* and Editor of *Asian J Phys*. Email: shantib@iitm.ac.in

